



**HAL**  
open science

## Effectiveness of corrosion inhibitors in simulated concrete pore solution

Ahmed Elshami, Stéphanie Bonnet, Abdelhafid Khelidj, Latefa Sail

► **To cite this version:**

Ahmed Elshami, Stéphanie Bonnet, Abdelhafid Khelidj, Latefa Sail. Effectiveness of corrosion inhibitors in simulated concrete pore solution. *European Journal of Environmental and Civil Engineering*, 2018, pp.1-21. 10.1080/19648189.2018.1500309 . hal-01923528

**HAL Id: hal-01923528**

**<https://hal.science/hal-01923528>**

Submitted on 26 Nov 2018

**HAL** is a multi-disciplinary open access archive for the deposit and dissemination of scientific research documents, whether they are published or not. The documents may come from teaching and research institutions in France or abroad, or from public or private research centers.

L'archive ouverte pluridisciplinaire **HAL**, est destinée au dépôt et à la diffusion de documents scientifiques de niveau recherche, publiés ou non, émanant des établissements d'enseignement et de recherche français ou étrangers, des laboratoires publics ou privés.

# Effectiveness of Corrosion Inhibitors in Simulated Concrete Pore Solution

A. ELSHAMI<sup>a,\*</sup>, S. BONNET<sup>b</sup>, A. KHELIDJ<sup>b</sup>, L. SAIL<sup>c</sup>

<sup>a</sup> Lecturer at Housing & Building National Research Centre, 87 El Tahrir St. Dokki – Giza, Egypt

Tel (33) 1-40-43-51-65 Fax (33) 1-40-43-54-98

<sup>b</sup> UBL, Université de Nantes, GeM, CNRS UMR 6183, 58 rue Michel Ange (BP420), 44606 Saint Nazaire Cedex,  
France

<sup>c</sup>EOLE Laboratory, Civil Engineering Department, Faculty of Technology, University Abou Bekr Belkaid,  
Chetouane BP 230, Tlemcen

## ABSTRACT

Steel embedded in concrete is normally in a passive state against corrosion due to a thin iron oxide layer that forms on the steel surface and remains stable in the high alkaline environment of the concrete. This protective film must be destroyed (depassivation) and this can be mainly done in two ways: by the attack of chlorides on the steel (seawater, de-icing salt, unwashed sea sand, admixtures etc.) or by carbonation. Corrosion inhibitors may be a good alternative to protection steel against corrosion due to its lower cost and easy application. Many researchers are inclined to use surface applied corrosion inhibitors and prefer to use the  $Cl^-$ /inhibitor parameter as an indication of chloride inhibitor threshold level. The objective of this study was to fill the gap left by public research in developing methods of corrosion control of reinforcement in concrete by synthetic solutions to emulate concrete environment. Three inhibitors were distinguished as passivation inhibitors in real solution extract and synthetic. In this study the tests with calcium nitrite (CNI), sodium monofluorophosphate (MFP) and ethanolamine based inhibitors showed reductions in the overall rates of corrosion after the inhibitive treatments.

### *Keywords:*

Concrete, Corrosion, Chloride, Carbon Steel, CNI, AMA and MFP.

---

\* Corresponding author. Tel.: +33-1-40-43-51-65; Fax: +33-1-40-43-54-98.  
E-mail address: materialhnbrc@yahoo.com (Ahmed. Elshami).

28  
29  
30  
31  
32  
33  
34  
35  
36  
37  
38  
39  
40  
41  
42  
43  
44  
45  
46  
47  
48  
49  
50  
51  
52  
53  
54  
55

## Effectiveness of Corrosion Inhibitors in Simulated Concrete Pore Solution

A. ELSHAMI<sup>a,\*</sup>, S. BONNET<sup>b</sup>, A. KHELIDJ<sup>b</sup>,

<sup>a</sup> Lecturer at Housing & Building National Research Centre, 87 El Tahrir St. Dokki – Giza, Egypt

58 Bd Lefebvre, F-75732 Paris Cedex 15, France

Tel (33) 1-40-43-51-65 Fax (33) 1-40-43-54-98

<sup>b</sup>GeM (UMR CNRS 6183) Institut de Recherche en Génie Civil et Mécanique IUT de Saint-Nazaire,

58 rue Michel Ange, B.P. 420, F-44606 Saint-Nazaire Cedex- France

### 1. Introduction

Minimising the direct and indirect costs of marine structure maintenance and maximising the available capacity is critical to the economic competitiveness of an expanding European Union. The use of corrosion inhibitors – a developing technology - as part of a repair strategy may provide a cost effective solution. A bibliography of over 180 references was assembled. A detailed review was made of material published in the last fifteen years. The review embraced some aspects of CNI, AMA and MFP based inhibitors, used in new construction and repair methods based on cementitious mortars but the main focus was on surface applied corrosion inhibitors. Several studies have been conducted to assess the effects of chloride ions in simulated pore solution. A summary of available literature was given to the most commonly used inhibitors such as CNI, AMA and MFP in artificial concrete pore solutions. In tests with calcium nitrite, sodium monofluorophosphate and ethanolamine based inhibitive treatments Monticelli et al (2000) [1] observed moderate reductions in the overall rates of corrosion after the inhibitive treatments. To ensure this effectiveness the ratio between

---

\* Corresponding author. Tel.: +33-1-40-43-51-65; Fax: +33-1-40-43-54-98.  
E-mail address: materialhnbrc@yahoo.com (Ahmed. Elshami).

56 inhibitors and chloride ions has to be relatively high (approximately 1) (Elsener et. al. 1999)  
57 [2]. Mammoliti et al (1999) [3] have shown that calcium nitrite addition into simulated pore  
58 solution at a level of 0.1% was able to repassivate pre-corroded steel in 1% chloride. When  
59 the chloride was added to the simulated pore solution already containing 0.1% calcium  
60 nitrite, the increase in chloride up to 1.5–2.0% did not change the potential or the  
61 corrosion rate significantly [Ngala, et al, 2002] [4]. However, CNI in solutions of very high  
62 pH value the concentration of  $\text{Ca}^{2+}$  ions is strongly limited by the solubility product of Ca  
63  $(\text{OH})_2$ . The presence of CNI in the pore solution leads to precipitate calcium hydroxide (and  
64 consequent reduction in pH) [Li et al, 2000] [5]. Kawamura et al (1997) [6] measured the  $[\text{Cl}^-]$   
65  $]/ [\text{NO}_2^-]$  ratio both in pore solution and in mortar specimens. The free chloride  
66 concentration in the pore solution decreased and the  $\text{OH}^-$  content increased with the  
67 time of aging. The  $[\text{Cl}^-]/[\text{NO}_2^-]$  ratio remained fairly constant and achieved a value of about  
68 0.8 for 0.5% of admixed NaCl and 1% of sodium or calcium nitrite. The best inhibiting  
69 capacity was noted when the inhibitor was introduced in the solution before the  
70 contamination with chlorides, what gave a reduced effect especially when chlorides were  
71 present in the simulated pore solution [Benzina et al, 2008] [7]. In salt solution the AMA-  
72 based inhibitor delayed the initiation of corrosion and reduced the  $I_{\text{corr}}$  (when the NaCl  
73 concentration is 0.3%,  $I_{\text{corr}}$  was 0.45 and  $0.1\mu\text{A}/\text{cm}^2$  for the control and the inhibitor  
74 samples, respectively) [Heiyantuduwa et al,2003] [8]. AMA inhibitors are best used to  
75 extend (or help to achieve) the required service life by deferring the initial time to  
76 depassivation, and/or through reducing the rate of corrosion once corrosion is propagated, or  
77 retard incipient action (ring anode) [9]. Passivation due to the amino inhibitor is reached by  
78 the formation of an adsorbed layer on the steel surface. When the critical concentration ratio  
79 is not reached, the layer is partly destroyed, and the corrosion damage is rather localized.  
80 When the stabilization of the passive state is reached due to the inhibitor and subsequently the

81 concentration of the inhibitor is reduced, the initiation of corrosion might reoccur (the ratio of  
82 concentrations inhibitor/ $\text{Cl}^-$  is critical also in such cases) [10]. The sooner the inhibitor is  
83 introduced after corrosion propagation the more effective it is [11]. The long-term  
84 concentration of the inhibitor near the reinforcement, which may decrease over time due to  
85 leaching and evaporation, is a crucial parameter for the effectiveness of the inhibitor as part of  
86 a repair strategy [12]. Monofluorophosphate seems slightly efficient in simulated pore solution  
87 and in mortar and higher MFP concentration being slightly better (0.05, 0.1 and 0.5 M MFP  
88 and 0.5 M NaCl) [Alonso, 1996] [13]. The effectiveness of MFP increases with the inhibitor  
89 concentration in alkaline solution [Hope and Thompson, 1995] [14] and the minimum  
90 efficient ratio MFP/ $\text{Cl}^-$  (0.5 M NaCl and 0.5 M MFP) is reported to be 1–1.5 [Lafave et  
91 al, 2002, Palmer and Malric, 2000] [15,16]. The aim of this work is study of the basic  
92 mechanism of inhibitors for corrosion control of reinforcement in concrete by tests in  
93 simulated concrete pore solution.

## 94 **2. Experimental program**

95  
96 This part consists of two methods based on influence of (CNI, AMA and MFP) inhibitors  
97 firstly, in simulated concrete pore solution and secondly, influence of AMA in extracted  
98 cement solution because AMA is claimed to inhibit corrosion by penetrating concrete and  
99 adsorbing on the metal surface more than CNI and MFP. The demonstrate AMA in extracted  
100 cement solution is new applied to evaluate the influence of inhibitors in blended cement  
101 extract solution. The laboratory tests in simulated concrete pore solution included exposure of  
102 steel specimens in pore solution with analysis of corrosion damage and passive layers;  
103 exposure of steel specimens in pore solution with chloride and analysis of corrosion damage;  
104 determination of potentiodynamic polarization curves in simulated pore solution;  
105 determination of electrochemical impedance spectra in simulated pore solution.

106 *2.1 Materials and methods*

107

108 In order to achieve the goals of this study several laboratory tests in simulated concrete pore

109 solution were performed. These were as follows:

110 • Exposure of steel specimens in solution with analysis of corrosion damage and passive  
111 layers,

112 • Exposure of steel specimens in artificial pore solutions with  $\text{Cl}^-$  and analysis of corrosion  
113 damage,

114 • Determination of open circuit potential  $E_{\text{OC}}$ , potentiodynamic polarization curves in  
115 simulated pore solution,

116 • Determination of electrochemical impedance spectra in simulated pore solution,

117 • Influence of AMA inhibitors in blended cement extract solution

118 Corrosion inhibitors, CNI, AMA and MFP were added to the different solutions

119 separately. The dosage of CNI is 300 ml/l and the dosage of AMA is 4% (v/v) which is

120 equivalent to (40 ml/l). In this work the dosage of MFP is 2% equivalent to (20g/l) and which

121 is below the recommended amount (5%) to check the inhibition effect in the corrosion

122 process. Experiments were conducted using carbon steel bars, and with a diameter of 8 mm),

123 reference steel. The inhibited steel surface was approximated as a cylinder with a height of 2

124 cm corresponding to a surface area of  $5.02 \text{ cm}^2$ . Each sample was allowed a period of 24

125 hours to stabilize in the solution before applying the test. Firstly, a saturated calcium

126 hydroxide solution (noted S1) has been used to simulate the aqueous alkaline content of the

127 (non-carbonated) concrete pore solution, with an approximate pH of 13. Secondly to

128 simulate the aqueous phase of a concrete contaminated with chloride, was used to obtain

129 an electrolyte designated by S2 (see Table 1). This contains  $\text{Ca}(\text{OH})_2$  saturated solution and

130  $\text{NaCl}$ . This chloride content is higher than critical threshold by approximately 20 times,

131 because most of the existing research generally agrees that the  $\text{Cl}^-/\text{OH}^-$  threshold ratio for

132 carbon steel is  $< 1$ . The initial pH measured was 13, but, it dropped to a value of  $12.5 \pm 0.05$   
133 due to the chloride addition and possible carbonation from air during poring into the  
134 corrosion cells (Nedal, 2009) [17]. The range was 3.5% for chloride concentration. In some  
135 experiments the inhibitor was added to the simulated pore solution (S1) at the very beginning,  
136 when the steel surface was still clean, to investigate delay of time to depassivation. In other  
137 experiments the inhibitor was added the simulated pore solution (S2) after the corrosion  
138 already started to investigate the influence on corrosion rate control. The results of the  
139 measurements obtained in simulated pore solution represent the basis for further  
140 investigations in concrete.

## 141 2.2 *Extracted cement solution*

142 This part is concentrated on the influence of AMA in extracted cement solution. Pore solution  
143 extract for a concrete mix of water to cement ratio of 0.4 is (Hydroxyl  $\text{OH}^-$ , 700 mmol,  
144 Sodium  $\text{Na}^+$ , 192 mmol, Potassium  $\text{K}^+$ , 592 mmol, Sulphate  $\text{SO}_4^{2-}$ , 44 mmol, Calcium  $\text{Ca}^{+2}$ ,  
145 2 mmol). The pH found in extracted cement solution is 13.7. The use of AMA in extracted  
146 cement solution is new applied in our laboratory. The inhibition efficiency of the AMA to the  
147 surface of six steel (repeatability for one test) placed in extract solutions more or less  
148 corrosive and simulating more or less degraded concrete was investigated through  
149 electrochemical methods Figures (1). Free corrosion potential measuring  $E_{OC}$ , Cyclic  
150 polarization test and potentiodynamic scan (GC) were applied after 1 day and 2 days up to 8  
151 days of immersion. Experiments were conducted using carbon steel bars, and with a diameter  
152 of 8 mm), reference steel.

153

## 154 2.3 *Electrochemical Measurements*

155 In order to apply the open circuit potential ( $E_{oc}$ ) of a metal, the potentiodynamic scan or the  
156 cyclic polarization scan, three electrodes are immersed in the testing solution and connected

157 to a Biologic Ec- Lab potentiostat a device that is used to apply on over potential and record  
158 the induced current. Potentiodynamic scan and cyclic polarization are similar to the Cyclic  
159 polarization test. These tests were applied after 1 day and 2days up to 8 days of immersion.  
160 The data obtained for each time from six steel (repeatability for one test). The electrochemical  
161 impedance is then automatically calculated from this data in lab measurements. The  
162 experiment is controlled by data logging system and analysis is done using software provided  
163 by the manufacturer.

### 164 *2.3.1 Open Circuit Potential Measurements EOC*

165 The free corrosion potential is a good indication of the metal's tendency to corrode in a  
166 certain solution. Having a relatively fixed (not drifting) potential is an indication that the  
167 sample has stabilized in the solution. The test parameters are:

- 168 • The total time: this is the test duration in seconds. The sample's potential was measured  
169 against the Saturated Calomel Electrode (SCE) for duration of 60 seconds.
- 170 • The sample period: this parameter determines the spacing between data points in  
171 seconds. The sample period was 1 second.
- 172 • The stability: that is used to tell the system the definition of a stable potential. When  
173 measuring the open circuit potential, if the drifting rate falls below the stability this will result  
174 in terminating the experiment immediately. This parameter has units of mV/sec. The stability  
175 was set to be zero mV/sec. This means that the test will be terminated only when the total  
176 time ends.
- 177 • Sample Area: the sample surface area in (cm<sup>2</sup>) that is immersed in the solution.

### 178 *2.3.2 . Potentiodynamic Scans*

179 The potentiodynamic scan was used to measure corrosion current density, and then corrosion  
180 rate was calculated. For every sample, the potentiodynamic scan was applied to determine the  
181 corrosion current density  $i_{corr}$  at that time. The test parameters are:

182 •Initial E: is the starting point for the potential sweep in Volts. The initial potential E was -100  
183 mV vs.  $E_{OC}$ .

184 •Final E: is the ending point for the potential sweep in Volts. The final potential E was 1000  
185 mV vs.  $E_{OC}$ . This scan range ( $E_{OC}$  from -100 to + 1000 mV) enabled the estimation of  $i_{corr}$   
186 without destroying the sample. Testing further anodic potentials would force the sample to  
187 corrode (i.e., destructive testing).

188 •The sample period: the sample period was 1 second.

189 •Scan Rate: is the speed of the potential sweep during data acquisition. Its unit is mV/sec.  
190 Very high scan rates lead to unreliable data; however, very low scan rate elongate the test  
191 period. The applied scan rate was 0.1 mV/sec.

192 •Density: is the density of the metal tested in  $g/cm^3$ . This parameter is used for corrosion rate  
193 calculation.

194 •Equivalent Weight: is the theoretical mass of metal that will be lost from the sample after one  
195 Faraday of anodic charge has been passed. This parameter is used in corrosion rate  
196 calculations.

197 •Initial Delay: this option is used to allow the open circuit potential of the sample to stabilize  
198 prior to the potential scan. The delay time is the time that the sample will be held at its open  
199 circuit potential  $E_{OC}$  prior to the scan. The delay may stop prior to the delay time if the  
200 stability criterion for  $E_{OC}$  is met. The delay time parameter is active only if the initial delay is  
201 turned on. This option was turned off in all the experiments.

202 •Extrapolation of the corrosion current density  $i_{corr}$  was made with the help of potentiostat  
203 Analyst software.

### 204 2.3.3 Cyclic polarization

205 Each sample was allowed a period of 24 hours to stabilize in the solution before applying the  
206 test. The test parameters are:

- 207 •Initial E: is the starting point for potential sweep; initial E was  $-0.025\text{ V}$  vs.  $E_{OC}$ .
- 208 •Final E: is the ending point for potential sweep; final E was  $+0.025\text{ V}$ . The forward  
209 scan rate was  $0.5\text{ mV/sec}$ . The test is used mainly to investigate the metal's tendency to  
210 pitting corrosion in a certain environment and this ratio may be reach to  $-600\text{ mV}$  to  $+600$   
211  $\text{mV}$  according to aggressive environment.
- 212 •Apex E: is the end potential for the anodic (upward) scan. Apex E ( $E_{rev}$ ) is one of two  
213 conditions that will terminate the forward sweep and initiate the reversal scan if it is reached  
214 and the Apex I is not exceeded yet. Apex E was one V vs.  $E_{OC}$ .
- 215
- 216 •Apex I: is the corrosion current density that is indicative of pitting initiation and it is one of  
217 two conditions that will terminate the forward sweep and initiate the reversal scan if it is  
218 exceeded by the absolute current of the sample. The Apex I was  $1\text{ }\mu\text{A/cm}^2$ .

#### 219 2.3.4 Electrochemical Impedance Spectroscopy (EIS):

220 Literature on the applications of EIS shows that it has great advantages over other techniques  
221 in studying the passive film formation providing the use of low frequencies of AC signal  
222 [Pruckner, 2001] [18]. The test parameters are:

223 Initial Frequency: is the starting point for the frequency sweep during the data acquisition  
224 phase. The frequency unit is Hertz. The initial frequency was  $100\text{ kHz}$ .

225 Final Frequency: is the ending point for the frequency sweep during the data acquisition  
226 phase. The final frequency was  $100\text{ mHz}$  for cathodic electrochemical treatment and  $50\text{ mHz}$   
227 for inhibitor treatment. Testing lower frequencies would make the test duration too long.

228 Points/decade: is the number of data points in each decade frequency. The value used was the  
229 default value of  $70-90$  points per decade.

230 AC Voltage: is the amplitude of the applied AC (alternated current) signal to the working  
231 electrode. The unit is in root mean square (rms) mV. The excitation AC signal should be  
232 small in order to keep in the linear region (i.e., the AC current response will be in the same

233 frequency but with phase shift) and not to destroy the sample. The applied AC voltage was 10  
234 mV rms.

235 DC Voltage: is the applied DC (direct current) voltage on the working electrode. The purpose  
236 of the experiment was to study the properties of the passive film that is formed naturally on  
237 the metal surface. Thus, samples were held at their free corrosion potential EOC (i.e., DC  
238 Voltage = 0.0 vs. EOC).

239 Estimated Z: is a rough estimate of the cell's impedance at the Initial Frequency entered. This  
240 value is used to minimize the number of trials that the  
241 system operates to calculate the cell's impedance at the first data point. After the first point,  
242 this value is not important as the system uses the last estimated value for Z to calculate the  
243 new Impedance with the new frequency.

244 Figure 2a shows a schematic of the equivalent circuit R(QR) for non treated steel used in EIS  
245 data fitting. The proposed electric equivalent circuit  $R_{el}+C_f/R_f+C_{dl}/R_{ct}$  for steel treated with  
246 inhibitors by [Nedal, 2009 and Pruckner 2001 [17, 18] in their work to study passive film  
247 formation on carbon steel in alkaline solutions is given in Figure 2b. This circuit consists of  
248 the solution ohmic resistance  $R_{el}$  connected in series to two loops. The first loop represents  
249 the double layer capacitance  $C_{dl}$  and the charge transfer resistance  $R_{ct}$ . The other loop  
250 represents the passive film formed on steel surface in the high alkaline solutions where  $C_f$  and  
251  $R_f$  are the faradic capacitance and the ohmic resistance of the film, respectively. It is believed  
252 that this circuit introduces a reasonable explanation of the ongoing electrochemical process on  
253 the metal surface immersed in a high alkaline solution.

254 Since the capacitance (c) equals the charge built up in the capacitor (q) divided by the  
255 potential (V) (the free corrosion potential in this case), a metal in a passive state (i.e. less  
256 metal dissolution-less charge transfer between the metal surface and the electrolyte) will have  
257 less capacitance than an actively corroding metal. In other words, for a constant exposed area

258 an active corrosion process will lead to an increase in the total charge transfer, which leads to  
259 increased film capacitance [Nedal, 2009,Sahoo and Balasubramaniam 2008] [17, 19].

260 This electrochemical impedance of the system presented in the following equations.

261 The impedance  $Z$  of a resistor equals:

$$262 \quad Z = R \quad [5.1]$$

263 Where  $R$  is the resistance in ohms.The impedance of a capacitor equals:

$$264 \quad Z = \frac{1}{j\omega C} \quad [5.2]$$

265 Where  $C$  is the capacitance in farads,  $j$  is  $\sqrt{-1}$  and  $\omega$  is the angular frequency  $\omega = 2\pi f$ .

266 The total impedance of a system  $Z_{total}$  when the components are connected in series equals:

$$267 \quad Z_{total} = Z_1 + Z_2 \quad [5.3]$$

268 The total impedance of a system  $Z_{total}$  when the components are connected in parallel equals:

$$269 \quad Z_{total} = \frac{Z_1 Z_2}{Z_1 + Z_2} \quad [5.4]$$

270 Thus, the total impedance equals:

$$271 \quad Z_{total} = R_{el} + \frac{R_f}{1 + R_f(j\omega C_f)} + \frac{R_{ct}}{1 + R_{ct}(j\omega C_{dl})} \quad [5.5]$$

272 Where

273  $R_{el}$ : resistance of electrolyte

274  $R_f$ : film resistance formed in alkaline solution

275  $R_{ct}$ : charge transference resistance

276 The other loop represents the passive film formed on steel surface in the high alkaline  
277 solutions where  $C_f$  and  $R_f$  are the faradic capacitance and the ohmic resistance of the film,  
278 respectively.

279 A capacity film reduction ( $C_f$ ) that leads to a film thickness increase (equation (5.6))

$$280 \quad \text{expressed as } C_f = \epsilon_o \epsilon_r A/d \quad [5.6]$$

281 Where  $\epsilon_0$  is the vacuum permittivity ( $8.85 \times 10^{-14}$  F cm<sup>-1</sup>),  $\epsilon_r$  is the dielectric constant  
282 ( $\approx 1$ ), A the active surface and d the thickness of film.

#### 283 2.4 SEM and EDS analysis.

284 To characterize the influence of coating in protection of steel from corrosion, SEM reveals the  
285 morphology and composition of film on the surface of steel created by inhibitive treatments in  
286 simulated concrete pore solution. The overall analysis SEM and EDS has identified the  
287 elements on surface of steel treated by inhibitors.

288

### 289 3. Results and discussion

#### 290 3.1 Results of Carbon Steel Immersed in Synthetic Solutions Emulating Concrete Admixed 291 with Inhibitors Open circuit potential.

##### 292 3.1.1 Open circuit potential

293 Fig. 3 shows the open circuit potential (also referred to the rest potentials) test obtained from  
294 linear polarizatón tests for carbon steel samples immersed in synthetic concrete pore solutions  
295 S1 as after 1 hour, until 8 days of immersion. Each point in this figure is the average of six  
296 points. At the first hours of the addition of inhibitors the rest potentials  $E_{OC}$  are respectively  
297 around -100 mV for the CNI, -460 for MFP in comparison with S1 without inhibitors and -  
298 330 mV for AMA. Guidance for interpretation of results is given in the ASTM standard  
299 C876-99[20] and is summarized in Table 2. The systems showing potentials lesser negative  
300 than -276 mV versus SCE are treated as passive systems and systems showing more negative  
301 than -276 mV versus SCE are treated as active. Thus, the rebars in S1+ CNI are probably  
302 passive whereas an active corrosion probably takes place on the rebars in S1 without inhibitor  
303 and with MFP. The rest potentials increase with time. Eight days after addition of inhibitors,  
304 the rest potentials  $E_{OC}$  of S1+CNI are respectively between -50 and -20 mV and between -  
305 220 and -330 mV for all inhibitors added in S1. These results indicate adsorption of an  
306 inhibitor film on the iron surface which leads to a slowdown of the corrosion probability after

307 the inhibitor addition. The potential of steel without inhibitors increases due to the presence of  
308 passive layer of oxides ( $\text{Fe}_3\text{O}_4$  and  $\text{Fe}_2\text{O}_3$ ) on the surface of steel.

### 309 3.1.2 Corrosion current evolution

310 The corrosion currents obtained from applying cyclic polarization curves for S1+CNI,  
311 S1+AMA and S1+MFP are illustrated in Figure 4. According to RILEM studies [Andrade et  
312 al. 2004] [21], 4 ranges of corrosion activity can be distinguished from negligible, to weak, to  
313 moderate and up to high Table.3. Each point of the corrosion current in this figure is the  
314 average of six points. After addition of inhibitor, the data shows lower corrosion currents with  
315 time and after 8 days the corrosion current range is from 0.12 to 0.46  $\mu\text{A}/\text{cm}^2$  for S1+CNI,  
316 S1+AMA respectively. For rebar S1+MFP, corrosion activity after 8 days is (3.5  $\mu\text{A}/\text{cm}^2$ ). In  
317 cases, S1+CNI, S1+AMA, the corrosion activity is constant with time. For S1 without  
318 inhibitor and MFP the current also is almost constant and more than 1  $\mu\text{A}/\text{cm}^2$  corresponding  
319 to high rate corrosion. So the corrosion process is probably slowed down but not stopped with  
320 S1+MFP. The order of  $I_{\text{corr}}$  from high to weak is: S1 = S1+MFP, S1+AMA > S1+CNI.

### 321 3.1.3 EIS measurements in pore solution

322 The electrical parameters ( $C_{\text{dl}}, R_{\text{ct}}$ ) obtained through fitting EIS data, using the electric  
323 equivalent circuit R(QR) and  $R_{\text{el}}+C_{\text{f}}/(R_{\text{f}}+C_{\text{dl}}/R_{\text{ct}})$ , are listed in (Table 4). The values of  $E_{\text{pit}}$  in  
324 table 4 illustrate that inhibitors increase the pitting resistance of the metal. EC-Lab software  
325 was used in data fitting. The mathematical method used was Levenberg- Marquardt method.  
326 Figure 5 shows a Nyquist plot of the impedance of carbon steel immersed in fresh concrete  
327 pore solution with various amounts of inhibitors added to the solution in a period of 8 days. It  
328 can be noticed that the low frequency portion of the impedance spectra (on the right hand  
329 side) increases with presence of inhibitor in the solution as a sign of passivity does not break  
330 down. Figure 5 shows the main conclusions for all types of inhibitors, the order of inhibition  
331 is: S1+AMA > S1+CNI > S1+MFP > S1 according to the values of  $R_{\text{ct}}$ .

332 In the Nyquist impedance two time constants (one at high frequency HF and another at low  
333 frequency LF) for treated steel, and thus the capacitive loop observed in the Nyquist plots is  
334 consisted of two non-decoupled capacitive loops just for CNI. For the carbon steel film, the  
335 double layer capacitance  $C_{dl} < 2.5 \mu\text{F}/\text{cm}^2$  shows that a small part  $R_{ct}$  of the inhibited steel  
336 surface is involved in the electrochemical reactions at the steel/solution interface [Simescu  
337 and Idrissi, 2009] [22]. The corrosion reaction occurs only on a very small fraction of the total  
338 inhibitor steel area.

339 Basically, the passive film has a high resistivity with inhibitors; however, it decreased with  
340 reference specimens in the solution S1. The inhibitor layer of iron oxides/hydroxides surface  
341 film seems to cover the entire surface blocking the active sites and the total impedance of the  
342 system increases continuously. Thus, the increase in the sum of the charge transfer resistance  
343 and the film resistance ( $R_{ct} + R_f$ ) was observed in Table 4. The faradic capacitance of the  
344 passive film  $C_f$  decreased with inhibitors addition to the solution due to the decrease of charge  
345 transfer at the metal/electrolyte interface and reduction of capacity film ( $C_f$ ) that leads to a  
346 film thickness increase. It is remarkable that the film capacitance MFP decreased by about six  
347 times than AMA and by three times than CNI.  $R_f$  and  $C_f$  are absent in diagrams corresponding  
348 to reference specimens immersed in alkaline solution, during only 8 days, due to the 8 days is  
349 not enough formation film on the surface of steel and also absence of inhibitors.

#### 350 3.1.4 Cyclic polarization curve

351 It can be noticed that the metal had a passive region (decreased applied over potential and  
352 current density) that started immediately after the Tafel area ( $E_{OC} \pm 50 \text{ mV}$ ) for CNI and  
353 between  $-220$  and  $-400 \text{ mV}$  for all inhibitors added in S1 and continued until  $E_{pit}$  was reached  
354 Figure 6. The results of  $E_{pit}$  are shown in Table 4. In these solutions, the hysteresis loop was  
355 determined but  $E_{rev}$  seems adherent because corrosion inhibitors are not used to totally stop  
356 corrosion and  $E_{pit}$ , which is an indication that the metal is re-passivate and able to resist pitting

357 corrosion at these inhibitors types. In addition, the recorded  $i_{\text{corr}}$  of MFP in reverse scan is  
358 higher than other inhibitors. Perhaps a longer exposure time in that solution with MFP was  
359 needed to increase the pitting resistance of the metal.

### 360 3.1.5 Surface analysis with SEM

#### 361 a). SEM of carbon steel in S1+MFP

362 Figure 7b shows the SEM on the surface of the samples immersed during 1 week in solutions  
363 S1 with MFP inhibitor. The inhibiting action of sodium phosphate showed that phosphate  
364 compounds form a protective layer on the steel surface when immersed in alkaline solution  
365 without chlorides. A passive layer of  $\text{Fe}_3\text{O}_4$ ,  $\gamma\text{-Fe}_2\text{O}_3$  and  $\text{FePO}_4 \cdot \text{H}_2\text{O}$  results of hydrolysis  
366  $\text{Na}_2\text{PO}_3\text{F}$  in aqueous and neutral media to form orthophosphate and fluoride [Alonso et al,  
367 1996] [13]. But phosphate compounds characterized by spherical glassy plate of sand rose,  
368 lamellar shapes crystal exists on the surface of steel.

#### 369 b). SEM of carbon steel in S1+AMA

370 The surface of the samples immersed during 1 week in solutions with inhibitor is depicted in  
371 Figure 7c. The one zoom images shows the presence of an oxide film due to displacement of  
372 the first hydrated monolayers of the iron oxide film. Smialowska et al (1981) [23] on the other  
373 hand, showed that the passive films formed in alkaline solutions are closer to an iron ox-  
374 hydroxide ( $\text{FeOOH}$ ) than to  $\gamma\text{-Fe}_3\text{O}_4$  or  $\text{Fe}_2\text{O}_3$  Smialowska et al (1985) [24]. The uniform  
375 film deposited over the surface and practically there are no signs of corrosion. The film  
376 becomes much thicker, more uniform and amino compounds are present on its surface. This  
377 behaviour is according to the literature, which suggests that the organic inhibitors usually  
378 adsorb on the surface leading to the formation of a thin adsorbed layer [Jamil et al. 2003] [25].  
379 The SEM observations show that the (N-CH bonds) is compact well crystallized and covers  
380 completely the steel surface. The film observed in big area characterized by eggs shape or  
381 cotton-balls shaped due to its big thickness. These positive charged groups are likely to form

382 at the expense of inhibitor interaction with water molecules (from hydrated layers  
383 compounds) on the iron surface [Jamil et al, 2003] [25]..

#### 384 *c). SEM of carbon steel in S1+CNI*

385 The results of influence of CNI on microstructure are shown in Figure 7d. A stable passive  
386 layer of  $\gamma$ -FeOOH is formed on the surface of steel. This film is insoluble in aqueous alkaline  
387 solution and creates a solid layer on steel surface blocking the transport of ferrous ions into  
388 the electrolyte. As can be seen from Figure 7d mixture of flower-like pattern of  $\alpha$ -FeOOH  
389 (goethite) and  $\gamma$ -FeOOH (lepidocrocite) and plate-shaped of calcium hydroxide are  
390 presented [Soylyev and Richardson, 2008] [26]. The inner layer composed mainly of magnetite  
391 is compact, dense and adherent.

392 Results of Carbon Steel Immersed in Synthetic Solutions Emulating Concrete Admixed with  
393 Inhibitors Open circuit potential

### 394 *3.2 Results of Carbon Steel Immersed in Synthetic Solutions Emulating Concrete Admixed* 395 *with Inhibitors under Chloride Ion Attack.*

#### 396 *3.2.1 Open circuit potential*

397 Figure 8 shows the open circuit potential in case of pore solution admixed with inhibitors  
398 under amount of chlorides 35 g/l. The rest potential value for S2 decreases significantly after  
399 8 days (due to the presence of chloride). A drop in the corrosion potential was happened by  
400 other researchers as an indication of reaching the critical chloride limit [Hausmann, 1967 and  
401 Li and Sagues, 2001] [27,28]. For S2+MFP and S2+AMA the rest potential has  
402 approximately the same value and increases with time. This result due to two reasons: the first  
403 reason is the competition between chloride and the film of inhibitor which leads to increase  
404 resistivity of the film. The second reason is that protonated amino group's bind chloride so the  
405 concentration of chloride required for initiation of corrosion. This is an important feature  
406 when the inhibitor is used in concrete structures, since it may help to increase the  $Cl^-/OH^-$   
407 threshold ratio, which is one of the more important parameters in controlling the corrosion in

408 reinforced concrete structures [Jamil et al, 2003] [25]. AMA is recommended as  
409 complementary technique for reduction in time of regeneration of the passivity is obtained.  
410 CNI is not affected by presence of chloride see Figure 8

### 411 3.2.2 Corrosion current evolution

412 Figure 9 shows the corrosion current density ( $i_{\text{corr}}$ ) obtained from carbon steel samples  
413 immersed in S2. With time, the corrosion currents for S2+CNI remain low and closed to  
414 values obtained with no chloride. The previous result indicates that calcium nitrite not  
415 affected by the presence of chloride and this due to that nitrite does not incorporate into the  
416 passive film, but reacts with the anodic corrosion products in the early stage competing with  
417 the chloride ions and hydroxide ions. It helps to repair the flaws, which are caused by chloride  
418 dissolution of the oxide film to the soluble chloro complexes of iron [El-Jazairi and Berke,  
419 1992 and Berke and Weil, 1994] [29,30]. But S2+AMA and S2+MFP show corrosion current  
420 which is decreasing with time and ranging from 2.5 to 7.5  $\mu\text{A}/\text{cm}^2$  at 8 days, indicating a  
421 lower corrosion activity of the rebars. Each sample needs enough time to whether develop its  
422 passivation layer or actively corrode. For S2, the corrosion currents of rebars increase  
423 significantly with time because of the corrosion products.

424

### 425 3.2.3 EIS measurements in pore solution (Initiation of corrosion (prevention of 426 corrosion))

427 In this group of experiments the inhibitor was firstly added to the pure simulated pore  
428 solution, and afterward chlorides were successively added. The main goal of these  
429 experiments was to investigate whether the inhibitor additionally stabilizes the passive state of  
430 clean, already passivated steel surface. At the beginning, it can be seen in Figure 10 that the  
431 inhibitor increased the total electro-chemical impedance of the system, as well as changed the  
432 profile of the spectra. The significant reduction of the total impedance was observed when the

433 chloride concentration in pore solution reached a rather high value. From the measured  
434 spectra presented as Nyquist plots it can be seen that the inhibitor considerably changed the  
435 shape of the spectrum. It can be therefore concluded that the structure of the passive layer due  
436 to the inhibitor differs from the layer in pure pore solution. The electrical parameters are listed  
437 in (Table 5) at 8 days. EIS data for S2 containing CNI, AMA and MFP aged 8 days in the  
438 same aggressive solution. Calcium nitrite is an anodic inhibitor. It functions by oxidizing  
439 corrosion product - ferrous ions - to ferric ions that precipitate in the alkaline solution of the  
440 concrete and form a protective layer on the reinforcement. The precipitate functions as a film  
441 repair because the ferric ions are insoluble in aqueous alkaline solutions and block the transfer  
442 of ferrous ions into the electrolyte. This is data due to competition between the formation and  
443 local destruction of the film obtained by the slow inhibitor dissolution. This classical  
444 corrosion mechanism leads to the diminution of  $R_{ct}$  and to the increase of the double layer  
445 capacitance  $C_{dl}$  while  $R_f$  increases in comparison with S1. This evolution corresponds to the  
446 electrolyte diffusion into the film pores. The order of inhibition is: S2+CNI >S2+AMA  
447 >S2+MFP >S2 according to the values of  $R_{ct}$ .

448

#### 449 *3.2.4 . Cyclic polarization curve*

450 Figure 11 represent the potentiodynamic polarization curves of steel in S2 solution without  
451 and with CNI, AMA and MFP. A higher significant potential shift is observed between S2  
452 with inhibitor and the S2 without inhibitor. It can be noticed that the pitting potential for CNI  
453 equal to +200 mV vs. SCE and this help the metal to repassivate (heal) when the pitting  
454 potential is increase.

455 The increase of the passive current density for the film resistance is suggesting the presence  
456 of a protective homogeneous layer on the steel surface. S2+MFP lead to the anodic formation  
457 of a passive layer which contributes to the decrease of chloride aggressiveness. A drop in

458 polarization resistance is an indication of reaching the critical chloride limit [Trejo and Pillai,  
459 2004 and Qian et al., 2008] [31,32].

460 Perhaps a longer exposure time of MFP in the solution S2 was needed to increase the pitting  
461 resistance of the metal. At higher chloride concentrations of reference specimen S2, the  
462 pitting potential  $E_{pit}$  decreased to be -400 mV vs. SCE, and the hysteresis loop did not close.  
463 The results of  $E_{pit}$  are shown in Table 5. This is an indication of the breakdown of the passive  
464 film and that the metal was not able to repassivate (was not able to heal) at these chloride  
465 concentrations. This behaviour can be explained by the competitive action of both  $Cl^-$  and  
466  $OH^-$  ions in the solution [Naceur et al, 2007] [33].

467

### 468 *3.2.5 The charge transfer and film resistance*

469 Figure 12 and Figure 13 show an increase in the charge transfer resistance ( $R_{ct}$ ) and film  
470 resistance ( $R_f$ ) for all inhibitor more than the reference. However,  $R_f$  is equal to zero in Ref  
471 steel due to absence of inhibitors even with and without of  $Cl^-$  ions in the solution, this  
472 behaviour may be due to the time (8days) no sufficient for formation of film on the surface of  
473 steel. The order of inhibition when immersed in S1 is: AMA >CNI >MFP >Ref steel  
474 according to the values of  $R_{ct}$ , this meaning that AMA is more active in absence of  
475 chloride. The order of inhibition is: CNI >AMA >MFP >Ref steel according to the values of  
476  $R_{ct}$  and  $R_f$  when immersed in S2, this meaning that CNI is more active in presence of chloride.  
477 Basically, the passive film has a higher resistivity with CNI, AMA and MFP than the  
478 reference in pore solution S2 due to competition between chloride and the film of inhibitors  
479 which act as mechanical barrier against corrosion. MFP seems slightly efficient in simulated  
480 pore solution and slightly lower with NaCl.

### 481 *3.2.6 Surface analysis with SEM*

482 *a). SEM of carbon steel in S2+MFP*

483 The SEM shows that the pitting was observed on the sample Figure 14b. The brighter surface  
484 in SEM microphotographs exhibit pits that appeared darker in optical microphotographs. The  
485 pits appeared to occur only on sharply faceted grains. This indicates the accumulation of salts  
486 of phosphorus, chloride and calcium in the pits. The cracks have higher phosphorus content  
487 and exhibited the deposition of corrosion products.

488 *b). SEM of carbon steel in S2+AMA*

489 In figure 14c the SEM observations show the presence of a great amount of corrosion  
490 products like balloons swell and spread over the entire layers of the film surface.

491 It is suggested [Smialowska et al.1985 and 1981] [23,24] that the presence of chlorides in the  
492 solution changes the composition, thickness, and density of the passive film. Some author's  
493 report that the film formed in the presence of chlorides becomes thicker, but more porous and  
494 hydrated, losing its protective character [Jamil HE et al. 2005] [34].

495 The negatively charged ions (chloride ion) could reflect an interaction with the protonated  
496 amino groups.

497 *c). SEM of carbon steel in S2+CNI*

498 In figure 14d the SEM observations show the presence of a white precipitate formed over  
499 surface. This precipitate was analysed using EDS (X-ray spectroscopy) and found to be  
500 predominantly calcium and oxygen, suggesting that it is most likely  $\text{Ca}(\text{OH})_2$ . However, full  
501 protection depends greatly on the concentration of aggressive ions such as the chloride ion.  
502 The free chloride concentration in the pore solution admixed with CNI decreased and the  $\text{OH}^-$   
503 content increased with the time of aging.

504 CNI is highly soluble in neutral solution. However, in solutions of very high pH value the  
505 concentration of  $\text{Ca}^{2+}$  ions is strongly limited by the solubility product of  $\text{Ca}(\text{OH})_2$ . The  
506 presence of CN in the pore solution causes part of its  $\text{Ca}^{2+}$  ions to react with the  $\text{OH}^-$  ions in  
507 the solution to precipitate calcium hydroxide [Li et al, 2000] [5].

508 3.3 Corrosion behaviour in solution extract of blended cement.

509

510 3.3.1 Results of Carbon Steel Immersed in Solutions Extract of blended Cement

511 Admixed with AMA

512 In the recent years, there are few studies using AMA in advanced types of blended cement  
513 concrete. So this new study focused only on using ethanolamine in extract pore solution of  
514 blended cement.

515

516 a). Open circuit potential

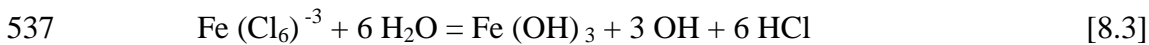
517 Figure 15 shows the open circuit potential tests for carbon steel samples immersed in solution  
518 extract of cement without chloride (EC) and solution extract of cement with chloride 35 g/l  
519 added to the solution (ECC). After 8 days the rest potentials  $E_{OC}$  are almost constant with time  
520 respectively around -250 mV for the EC+AMA and -330 mV for EC. According to ASTM  
521 (C876) the rebars in EC+ AMA are probably passive. These results indicate adsorption of  
522 passive film on the iron surface.

523 For ECC, after eight days, the rest potential values are higher until 6 days then decrease. This  
524 means that the corrosion conditions are in risk range.

525 b). Corrosion current evolution

526 The corrosion currents are illustrated in Figure 16. After addition of inhibitor, the data  
527 shows lower corrosion currents with time and after 8 days the corrosion current range is from  
528 4.5 to 3.9  $\mu\text{A}/\text{cm}^2$  for EC+AMA. It is to be noticed that this corrosion current constant with  
529 tendency of steel to corrode, which could be considered as an efficiency indicator for the  
530 inhibitor treatment according to RILEM studies [Andrade et al. 2004] [21]. In case of EC and  
531 EC+AMA the corrosion activity is constant. In case, of extract solution ECC without  
532 inhibitor, under amount of chlorides 35 g/l gives corrosion activity increase with time and  
533 those obtained from extract solution with inhibitor ECC+AMA decrease due to presence of  
534 amino inhibitors and this results agree with [Qian et al, 2008] [32]. The ECC behaviour can

535 be explained by lowering of pH by competitive action of both  $\text{Cl}^-$  and  $\text{OH}^-$  ions in the solution  
536 (see equation [8.3]).



538 *c). EIS measurements in pore solution*

539 Figure 17 shows a Nyquist plot of the impedance for carbon steel samples immersed in  
540 solution extract of cement with and without chloride in presence of AMA.

541 The electrical parameters obtained through fitting EIS data, using the electric equivalent  
542 circuit  $R(\text{QR})$  and  $R_{\text{el}} + C_f / (R_f + C_{\text{dl}} / R_{\text{ct}})$ , are listed in Table 6. From these diagrams low values  
543 of  $C_f$  and  $C_{\text{dl}}$  are recorded. The increase in the sum of the charge transfer resistance and the  
544 film resistance ( $R_{\text{ct}} + R_f$ ) was observed was adding of AMA.

545 For ECC, an increase in the sum of the charge transfer resistance and the film resistance ( $R_{\text{ct}} +$   
546  $R_f$ ) was observed with AMA. It is remarkable that the film capacitance of AMA increased by  
547 about three times from the beginning in EC of the experiment AMA ( $C_f$   $27.6 \mu\text{F}/\text{cm}^2$ ) until a  
548 chloride concentration in the solution ECC of  $35\text{g}/\text{l}$  ( $C_f$   $80 \mu\text{F}/\text{cm}^2$ ). AMA has great corrosion  
549 protection ability although it induced more chloride ion into the OPC concrete than BCC. This  
550 corrosion protection might be greatly attributed to the organic part in AMA around the rebar.  
551 The low frequency portion of the impedance spectra decreases in solution extract of cement in  
552 presence of chloride ion in the solution.

553  
554 Conclusions

555  
556 From the results presented in this paper it can be concluded that:

- 557 ■ Calcium nitrite (CNI), sodium monofluorophosphate (MFP) and ethanolamine (AMA)  
558 based inhibitors showed reductions in the overall rates of corrosion after the inhibitive  
559 treatments.

- 560   ▪ In alkaline solution with or without chloride, the CNI steel sample is more resistant than  
561   carbon steel alone and causing passivation of steel in concrete. Thus, a dense and  
562   protective layer is formed.
- 563   ▪ The laboratory study in simulated pore solution proved that all tests in simulated concrete  
564   pore solution proved that the amino alcohol inhibitor can reduce corrosion: the most  
565   important parameter is the ratio of inhibitor/chloride concentration,
- 566   ▪ if the steel reinforcement is heavily corroded the critical concentration ratio is strongly  
567   dependent on the steel surface conditions: after the initiation of corrosion this ratio must  
568   be quite high (e.g. 1:1) for the retardation of corrosion and if the steel is heavily corroded  
569   complete repassivation is practically impossible,
- 570   ▪ the efficiency of the inhibitor in solution with higher pH (simulated concrete pore solution  
571   without chlorides) cannot be exactly assessed, because the inhibitor shows a buffering  
572   effect,
- 573   ▪ passivation due to the inhibitor is reached by the formation of an adsorbed layer on the  
574   steel surface,
- 575   ▪ when the critical concentration ratio is not reached, the layer is partly destroyed, and the  
576   corrosion damage is rather localized (localized corrosion spots can be relatively deep),
- 577   ▪ when the stabilization of the passive state is reached due to the inhibitor and subsequently  
578   the concentration of the inhibitor is reduced, the initiation of corrosion might reoccur (the  
579   ratio of concentrations inhibitor/Cl<sup>-</sup> is critical also in such cases),
- 580   ▪ the sooner the inhibitor is introduced after corrosion propagation the more effective it is,  
581   ▪ it can be expected that the long-term concentration of the inhibitor near the reinforcement,  
582   which may decrease over time due to leaching and evaporation, is a crucial parameter for  
583   the effectiveness of the inhibitor as part of a repair strategy

- 584   ▪ Na<sub>2</sub>PO<sub>3</sub>F hydrolyses into the pore solution simulating the concrete to form phosphate and  
585   so anodic formation of passive layer contributes to the decrease of chloride  
586   aggressiveness.
- 587   ▪ The corrosion currents measured for solution extract of blended cement were  
588   significantly higher than those obtained at the same chloride concentration in the  
589   mortar and pore solution. It was found that the corrosion currents of carbon steel  
590   embedded in mortar immersion in NaCl at 3, 5%, would decrease due to the decrease  
591   in the degree of pore saturation PS after 28 days. Regardless in the presence of  
592   chloride content, the corrosion current was as low as 1, 5 μA/cm<sup>2</sup>
- 593   ▪ .

## 594   **References**

- 596   [1] C. Monticelli, A. Frignani, G. Trabanelli, (2000), “A study on corrosion inhibitors  
597   for concrete application”, *Cement and Concrete Research*, Vol. 30, pp. 635-642.
- 598   [2] B. Elsener, M. Buehler, Stalder, F., Böhni, H., (1999), “Migrating corrosion inhibitor  
599   blend for reinforced concrete: Part 1 – Prevention of corrosion”, *Corrosion*, Vol. 55,  
600   No. 12, pp. 1155-1163.
- 601   [3] Mammoliti L, Hansson CM, Hope BB. Corrosion inhibitors in concrete. Part II: effect  
602   on chloride threshold values for corrosion of steel in synthetic pore solutions. *Cem  
603   Concr Res* 1999;29:1583–9.
- 604   [4] Ngala VT, Page CL, Page MM. Corrosion inhibitor systems for remedial treatment of  
605   reinforced concrete. Part 1: Calcium nitrite. *Corr Sci* 2002;44:2073–87.
- 606   [5] Li Z.J., Ma B.G. Peng J. and Qi M., “The microstructure and sulfate resistance  
607   mechanism of high-performance concrete containing CNI”, *Cement & Concrete  
608   Composites*, 2000, 22, pp. 369-377.
- 609   [6] M Kawamura, S Tanikawa, RN Swamy, H Koto - Pore solution composition and  
610   electrochemical behavior of steel bars in mortars with nitrite. *ACI Special  
611   Publication*, 1997.
- 612   [7] L Benzina Mechmeche, L Dhouibi, M. Ben Ouedou, E. Triki, F.  
613   Zucchi. Investigation of the early effectiveness of an amino-alcohol based corrosion  
614   inhibitor using simulated pore solutions and mortar specimens. *Cement and Concrete  
615   Composites*, Volume 30, Issue 3, March 2008, Pages 167–173.

- 616 [8] Heiyantuduwa R, Beushausen HD, Alexander MG. The effectiveness of corrosion  
617 inhibitors in concretes subjected to chloride attack and carbonation. BFT 2003:8.
- 618 [9] L.Li, A.A.Sagues, , N.Poor, "In situ leaching investigation of pH and nitrite con-  
619 centration in concrete pore solution", Cement and Concrete Research, Vol. 29 (1999),  
620 pp. 315-321.
- 621 [10] L.Mammoliti, C.M., Hansson, B.B. Hope, "Corrosion inhibitors in concrete, Part II:  
622 Effect on chloride threshold values for corrosion of steel in synthetic pore solutions",  
623 Cement and Concrete Research, Vol. 29, (1999), pp. 1583-1589.
- 624 [11] J.Olek, , F.Martin, "Influence of corrosion inhibitors on the electrochemistry of cor-  
625 rosion processes of reinforcing steel in simulated pore solutions", Proceedings,  
626 Conference on Materials Problems in Civil Engineering, Cracow, (1996), pp. 302-  
627 309.
- 628 [12] N.R. Short, , P.Lambert, , C.L. Page, , "Effect of corrosion inhibitors on pore solution  
629 chemistry of hardened cement pastes", Proceedings, Second International Seminar on  
630 Durability of Concrete: Aspects of Admixtures and Industrial By-Products (editors:  
631 Berntsson, L.,Chandra, S., Nilsson, L.), Swedish Council for Building Research,  
632 Document D9-1989, (1989) pp. 218-228.
- 633 [13] Alonso C, Andrade C, Argiz C, Malric B. Na<sub>2</sub>PO<sub>3</sub>F as inhibitor of corroding  
634 reinforcement in carbonated concrete. Cem Concr Res1996;26(3):405–15.
- 635 [14] Hope BB, Thompson SV. Damage to concrete induced by calcium nitrite. ACI Mater  
636 J 1995;92(5):529–31.
- 637 [15] Lafave JM, Pfeifer DW, Sund DL, Lovett D, Civjan SA. Using mineral and chemical  
638 durability-enhancing admixtures in structural concrete. Concr Int 2002(August):71–8.
- 639 [16] Palmer R, Malric B. Surface applied inhibitors: conditions for application and control  
640 of penetration. In: International congress on advanced materials, their processes and  
641 applications. Munich, Ger-many; 2000.
- 642 [17] Nedal Mohamed. "Comparative Study of the Corrosion Behaviour of Conventional Carbon  
643 Steel and Corrosion Resistant Reinforcing Bars. A Thesis Submitted for the Degree of Master  
644 of Science University of Saskatchewan. August 2009.
- 645 [18] Pruckner, F. (2001). ""Corro sion and Protection of Re inforcement in Concrete  
646 Measurements and Interpretation"." PhD thesis, University of Vienna.
- 647 [19] Sahoo, G., and Balasubramaniam, R. (2008). "On the corrosion behaviour of  
648 phosphoric irons in emulated concrete pore solu tion." Corrosion Science, 50(1), 131.
- 649 [20] ASTM Standard C876-99. "Standard Test Method for Half-Cell Potentials of  
650 Uncoated Reinforcing Steel in Concrete." ASTM International, West Conshohocken,  
651 PA, 1999, DOI: 10.1520/C0876-91R99, Www.Astm.Org. (1999).

- 652  
653 [21] Andrade C., Alonso A & Al., "Test method for on-site corrosion rate measurement of  
654 steel reinforcement in concrete by means of the polarization resistance method",  
655 RILEM TC 154-EMC: Electrochemical Techniques for Measuring Metallic  
656 Corrosion - Recommendations, Materials and Structures, Vol. 37, n°9, 2004, pp.623-  
657 643.
- 658 [22] Simescu F., Idrissi H., "Corrosion behaviour in alkaline medium of zinc phosphate  
659 coated steel obtained by cathodic electrochemical treatment", Corrosion Science. vol.  
660 51, n°4, 2009, p. 833–840.
- 661 [23] Smialowska Szlarska-H. Oranowska, Z. An electrochemical and ellipsometric  
662 investigation of surface films grown on iron in saturated calcium hydroxide solutions  
663 with or without chloride ions. Corrosion Science 21 (1981) 735.
- 664 [24] Smialowska. T Zakroczymski, Z Szklarska .Activation of the iron surface to  
665 hydrogen absorption resulting from a long cathodic treatment in NaOH solution -  
666 Journal of the Electrochemical Society1985.
- 667 [25] Jamil HE, Montemor MF, Boulif R, Shriiri A, Ferreire MGS. An electrochemical and  
668 analytical approach to the inhibition mechanism of an amino-alcohol-based corrosion  
669 inhibitor for reinforced concrete. Electrochim Acta 2003; 48:3509–18.
- 670 [26] So" ylev T.A, M.G. Richardson. Corrosion inhibitors for steel in concrete: State-of-  
671 the-art report. Construction and Building Materials 22 (2008) 609–.622
- 672 [27] Hausmann, D. A. (1967). "Steel corrosion in concrete - How does it occur." Materials  
673 Protection, 6(11), 19.
- 674 [28] Li, L., and Sagues, A. A. "Chloride corrosion threshold of reinforcing steel in  
675 alkaline solutions - Open-circuit immersion tests." Corrosion, 57(1), 19. (2001).
- 676 [29] El-Jazairi B., and Berke N.S., "the use of calcium nitrites as corrosion  
677 inhibiting admixture to steel reinforcement in concrete". Elsevier Science  
678 Publishers Ltd ., Wishaw, Warwickshire, UK. 1992.
- 679 [30] Berke, N.S., Weil, T.G., (1994), "World wide review of corrosion inhibitors in  
680 concrete" Ad-vances in Concrete Technology (editor: Malhotra, V.M.), CANMET,  
681 Montreal, pp. 891-914.
- 682 [31] Trejo, D., and Pillai, R. (2004). "Accelerated chloride threshold testing - Part II:  
683 Corrosion-resistant reinforcement." AC I Materials Journal, 101(1), 57
- 684 [32] Qian, S., Cusson, D., Chagnon, N., and Ba Idock, B. (2008). "Corrosion-Inhibiting  
685 systems for durable concrete bridges. II: A ccelerated laboratory investigation."  
686 Journal of Materials in Civil Engineering, 20(1), 29.
- 687 [33] Naceur Etteyeb, Leila Dhouibi, Mercedes Sanchez, Cruz Alonso, Carmen Andrade  
688 and Ezzeddine Triki. Electrochemical study of corrosion inhibition of steel

689 reinforcement in alkaline solutions containing phosphates based components  
690 Naceur Etteyeb, Journal of Materials Science Volume 42, Number 13 (2007), 4721-  
691 4730, DOI: 10.1007/s10853-006-0880-3

692 [34] Jamil HE, Shriri A, Boulif R, Montemor MF, Ferreira MGS. Corrosion behaviour of  
693 reinforcing steel exposed to an amino alcoholbased corrosion inhibitor. Cem Concr  
694 Com 2005;27(6):671–8.